J. Astrophys. Astr. (1993) **14,** 103–114

# Plasma Instability at the Inner Edge of the Accretion Disk—I

S. C. Tripathy, *Udaipur Solar Observatory, Udaipur, 313 001*
C. B. Dwivedi, *Institute for Plasma Research, Bhat, Gandhinagar, 382 424*
A. C. Das & A. R. Prasanna *Physical Research Laboratory, Navrangpura, Ahmedabad 380 009*

Received 1993 January 5; accepted 1993 April 16

**Abstract.** In this paper, the analytical and numerical results of the stability analysis of the accretion disk at the inner boundary is presented. Including the effect of finite conductivity in the disk dynamics, a simple calculation considering only the radial perturbation has been carried out. Within local approximation, it is concluded that the disk is stable to Kelvin-Helmholtz and resistive electromagnetic modes whereas the magnetosonic mode can destabilise the disk structure.

*Key words*: Accretion disks—hydromagnetics—instability

## 1. Introduction

Recent developments in the study of thick accretion disks around compact objects has stressed the inclusion of self-generated electromagnetic fields and pressure gradient forces in the dynamical equations governing the structure and stability of accretion disks (Prasanna 1991). Addition of electromagnetic forces brings the inner edge of the disk closer to the central object, thus enhancing the efficiency of the energy release. The presence of strong magnetic field defines the magnetosphere where the accretion flow is dominated by magnetic pressure. The radial distance where the magnetic pressure equals the fluid pressure of the accreting matter is defined as the magnetopause or the inner boundary. In case of steady state accretion, the total disk luminosity is found to be half of the accretion luminosity and the other half has to be released at the inner boundary or close to the stellar surface. In either case, the boundary layer plays a dominant role in the accretion process. If the energy is radiated at the inner boundary layer, then one has to understand different plasma processes that convert the gravitational energy into X-rays. On the other hand, if the energy has to be released close to the stellar surface then the boundary layer plays an important role in pushing the matter inside. For a theoretical interpretation of X-rays from binary sources, attention has been focused on the various physical processes and hydromagnetic instabilities that could arise as a result of the interaction between the magnetic field of a neutron star and matter in a thin Keplerian disk. Recently this interaction has attracted considerable attention with regard to the formation of binary radio pulsars, the origin of quasiperiodic oscillations from low mass X-ray binaries (Taam & van den Heuvel 1986) and observed time variation of the pulse periods of X-ray sources. This interaction which regulates the spin of the central object by transferring material and angular momentum from the disk could be a possible mechanism for spinning old pulsars to millisecond regime, In the case of AGN's,

Wiita (1985) pointed out that instabilities in the accretion disks could lead to multiple ways of inducing variabilities as for example release of large amounts of magnetic energy on the surface of the disk (Shields & Wheeler 1976). In this context, it is necessary to understand different instabilities that can arise in disks supported by the gas and magnetic pressure.

The investigation of the interaction between a thin Keplerian disk with the magnetosphere of a rotating neutron star has been started only recently. The existence of velocity jump between the disk material and the magnetosphere invariably indicates the presence of Kelvin-Helmholtz instability (Chandrasekhar 1961). In the context of field penetration into the magnetic disk, this instability was invoked by Ghosh & Lamb (1978) and by Scharlemann (1978). In the context of disk accretion, Anzer & Borner (1980,1983) have explored some further aspects of Kelvin-Helmholtz instability. Restricting the analysis to a purely hydrodynamic treatment and assuming equal sound speeds on both sides of the boundary, they found that the instability can grow to large amplitudes only within a narrow ring around the co-rotation radius. Subsequently, the analysis was extended to incorporate the magnetic field and allowed different sound speeds in the disk and magnetosphere. However, this study was restricted to a simplified planar geometry with constant density and constant magnetic field. Some other authors (Choudhury & Lovelace 1986; Pietrini & Toricelli-Ciamponi 1989; and Corbelli & Torricelli-Ciamponi 1990) have analysed Kelvin-Helmholtz and hydromagnetic instabilities to model extragalactic radio jets using ideal MHD equations.

In order to elucidate the importance of inhomogeneous magnetic field, finite conductivity of the plasma and the velocity shear which arise due to the differential rotation of the disk, we carry out a linear stability analysis of a plasma disk under the influence of gravitational, electromagnetic and centrifugal forces. The equilibrium model of such a plasma disk was recently given by Tripathy *et al.* (1990, hereinafter

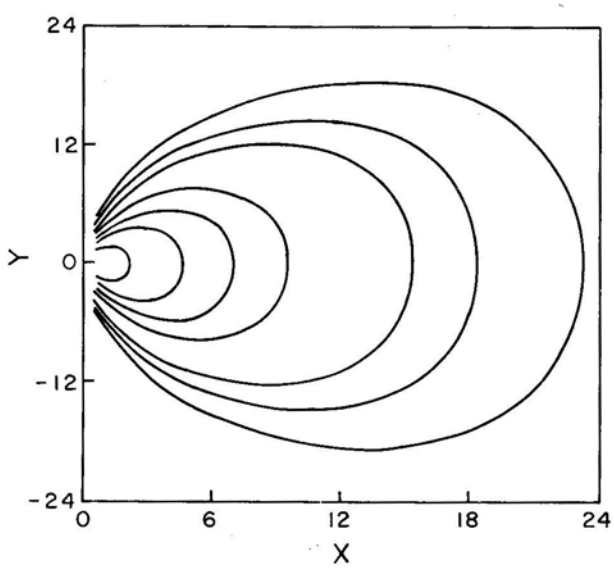


**Figure 1.** The magnetic lines of force projected on to the meridional plane of a disk around a compact object with a dipolar magnetic field.

referred to as paper I). In this configuration assuming the magnetofluid to be quasi-neutral, the effects of resistivity was taken through Ohm's law. The other main characteristics of this disk solution are the inclusion of self consistent magnetic fields and currents. Allowing the plasma to flow in all the three directions ($V_r, V_\theta, V_\phi$), it was concluded that there exists inter dependence between the magnetic moment of the central star and density and conductivity of the magneto-fluid. Further, from the turning point behaviour of the pressure profiles near the inner edge, it was postulated that instabilities would exist at the inner edge of the disk. However, the equilibrium magnetic field profile (Fig. 4 of paper I) shows discontinuous behaviour at the boundary of the disk. The discontinuity which arose due to the improper boundary conditions posed a problem on the stability of the equilibrium configuration itself. However, this discontinuity vanishes if we take into account proper boundary conditions (Fig. 1, also see Appendix A). This figure also ensures the continuity of the magnetic field lines at the boundary.

The plan of this paper is as follows. In section 2, we write down the perturbation equations explicitly and perform a stability analysis. The analytical and numerical results are presented in section 3 and conclusions are drawn in section 4.

## 2. Formalism

We consider small perturbations of the equilibrium solutions given in paper I. Expressing any physical quantity $\Psi = \psi + \tilde{\psi}$, where $\psi$ is the equilibrium part and $\tilde{\psi}$ is the generic perturbation such that $\tilde{\psi}/\psi \ll 1$, the linearised perturbation equations with the usual notation may be written as given below.

The linearised Maxwell's equations can be written as

$$\frac{1}{c}\frac{\partial \tilde{E}_r}{\partial t} - \frac{1}{r}\frac{\partial \tilde{B}_\phi}{\partial \theta} - \frac{\cot\theta}{r}\tilde{B}_\phi + \frac{1}{r\sin\theta}\frac{\partial \tilde{B}_\theta}{\partial \phi} + 4\pi\sigma c^{-2}[c\tilde{E}_r + \tilde{B}_\phi V_\theta - \tilde{B}_\theta V_\phi - B_\theta \tilde{V}_\phi] = 0, \tag{2.1}$$

$$\frac{1}{c}\frac{\partial \tilde{E}_\theta}{\partial t} + \frac{\partial \tilde{B}_\phi}{\partial r} + \frac{\tilde{B}_\phi}{r} - \frac{1}{r\sin\theta}\frac{\partial \tilde{B}_r}{\partial \phi} + 4\pi\sigma c^{-2}[c\tilde{E}_\theta + \tilde{B}_r V_\phi - \tilde{B}_\phi V_r + B_r \tilde{V}_\phi] = 0, \tag{2.2}$$

$$\frac{1}{c}\frac{\partial \tilde{E}_\phi}{\partial t} + \frac{1}{r}\frac{\partial \tilde{B}_r}{\partial \theta} - \frac{\tilde{B}_\theta}{r} - \frac{\partial \tilde{B}_\theta}{\partial r} + 4\pi\sigma c^{-2}[c\tilde{E}_\phi - \tilde{B}_r V_\theta + \tilde{B}_\theta V_r + B_\theta \tilde{V}_r - B_r \tilde{V}_\theta] = 0, \tag{2.3}$$

$$\frac{1}{c}\frac{\partial \tilde{B}_r}{\partial t} + \frac{1}{r}\left(\frac{\partial \tilde{E}_\phi}{\partial \theta} + \cot\theta\,\tilde{E}_\phi\right) - \frac{1}{r\sin\theta}\frac{\partial \tilde{E}_\theta}{\partial \phi} = 0, \tag{2.4}$$

$$\frac{1}{c}\frac{\partial \tilde{B}_\theta}{\partial t} - \frac{\tilde{E}_\phi}{r} - \frac{\partial \tilde{E}_\phi}{\partial r} + \frac{1}{r\sin\theta}\frac{\partial \tilde{E}_r}{\partial \phi} = 0, \tag{2.5}$$

$$\frac{1}{c}\frac{\partial \tilde{B}_\phi}{\partial t} + \frac{\tilde{E}_\theta}{r} + \frac{\partial \tilde{E}_\theta}{\partial r} - \frac{1}{r}\frac{\partial \tilde{E}_r}{\partial \theta} = 0. \tag{2.6}$$

The linearised momentum equations are given by

$$\frac{\partial \tilde{V}_r}{\partial t} + V_r\frac{\partial \tilde{V}_r}{\partial r} + \tilde{V}_r\frac{\partial V_r}{\partial r} + \frac{V_\theta}{r}\frac{\partial \tilde{V}_r}{\partial \theta} + \frac{\tilde{V}_\theta}{r}\frac{\partial V_r}{\partial \theta} + \frac{V_\phi}{r\sin\theta}\frac{\partial \tilde{V}_\phi}{\partial \phi} + \frac{\tilde{V}_\phi}{r\sin\theta}\frac{\partial V_\phi}{\partial \phi}$$
$$-\frac{2}{r}(V_\theta \tilde{V}_\theta + V_\phi \tilde{V}_\phi) + \frac{1}{\rho}\frac{\partial \tilde{P}}{\partial r} - \frac{\tilde{\rho}}{\rho^2}\frac{\partial P}{\partial r}$$
$$+\frac{1}{c\rho}[B_\phi \tilde{J}_\theta + \tilde{B}_\phi J_\theta - B_\theta \tilde{J}_\phi - \tilde{B}_\theta J_\phi + E_r \tilde{J}_t + \tilde{E}_r J_t]$$
$$-\frac{\tilde{\rho}}{c\rho^2}[E_r J_t + B_\phi J_\theta - B_\theta J_\phi] = 0, \tag{2.7}$$

$$\frac{\partial \tilde{V}_\theta}{\partial t} + V_r\frac{\partial \tilde{V}_\theta}{\partial r} + \tilde{V}_r\frac{\partial V_\theta}{\partial r} + \frac{V_\theta}{r}\frac{\partial \tilde{V}_\theta}{\partial \theta} + \frac{\tilde{V}_\theta}{r}\frac{\partial V_\theta}{\partial \theta} + \frac{V_\phi}{r\sin\theta}\frac{\partial \tilde{V}_\theta}{\partial \phi} + \frac{\tilde{V}_\phi}{r\sin\theta}\frac{\partial V_\theta}{\partial \phi}$$
$$+\frac{1}{r}(V_r \tilde{V}_\theta + \tilde{V}_r V_\theta - 2\cot\theta V_\phi \tilde{V}_\phi) + \frac{1}{r\rho}\frac{\partial \tilde{P}}{\partial \theta} - \frac{\tilde{\rho}}{r\rho^2}\frac{\partial P}{\partial \theta}$$
$$+\frac{1}{c\rho}[B_r \tilde{J}_\phi + \tilde{B}_r J_\phi - B_\phi \tilde{J}_r - \tilde{B}_\phi J_r + E_\theta \tilde{J}_t + \tilde{E}_\theta J_t]$$
$$-\frac{\tilde{\rho}}{c\rho^2}[E_\theta J_t + B_r J_\phi - B_\phi J_r] = 0, \tag{2.8}$$

$$\frac{\partial \tilde{V}_\phi}{\partial t} + V_r\frac{\partial \tilde{V}_\phi}{\partial r} + \tilde{V}_r\frac{\partial V_\phi}{\partial r} + \frac{V_\theta}{r}\frac{\partial \tilde{V}_\phi}{\partial \theta} + \frac{\tilde{V}_\theta}{r}\frac{\partial V_\phi}{\partial \theta} + \frac{V_\phi}{r\sin\theta}\frac{\partial \tilde{V}_\phi}{\partial \phi} + \frac{\tilde{V}_\phi}{r\sin\theta}\frac{\partial V_\phi}{\partial \phi}$$
$$+\frac{1}{r}[(V_r \tilde{V}_\phi + V_\phi \tilde{V}_r)] + \cot\theta(V_\theta \tilde{V}_\phi + V_\phi \tilde{V}_\theta) + \frac{1}{r\sin\theta\rho}\left(\frac{\partial \tilde{P}}{\partial \phi} - \frac{\tilde{\rho}}{r\rho}\frac{\partial P}{\partial \phi}\right)$$
$$+\frac{1}{c\rho}[B_\theta \tilde{J}_r + \tilde{B}_\theta J_r - B_r \tilde{J}_\theta - \tilde{B}_r \tilde{J}_\theta + \tilde{E}_\phi J_t$$
$$-\frac{\tilde{\rho}}{c\rho^2}[B_\theta J_r - B_r J_\theta] = 0. \tag{2.9}$$

The linearised perturbed continuity equation is given by

$$\frac{\partial \rho}{\partial t} + \rho\left[\frac{\partial \tilde{V}_r}{\partial r} + \frac{1}{r}\frac{\partial \tilde{V}_\theta}{\partial \theta} + \frac{1}{r\sin\theta}\frac{\partial \tilde{V}_\phi}{\partial \phi} + \frac{2\tilde{V}_r}{r} + \cot\theta\frac{\tilde{V}_\theta}{r}\right]$$
$$+\tilde{\rho}\left(\frac{\partial V_r}{\partial r} + \frac{1}{r}\frac{\partial V_\theta}{\partial \theta} + \frac{2V_r}{r} + \cot\theta\frac{V_\theta}{r}\right)$$
$$+V_r\frac{\partial \tilde{\rho}}{\partial r} + \frac{V_\theta}{r}\frac{\partial \tilde{\rho}}{\partial \theta} + \frac{V_\phi}{r\sin\theta}\frac{\partial \tilde{\rho}}{\partial \phi}$$
$$+\tilde{V}_r\frac{\partial \rho}{\partial r} + \frac{\tilde{V}_\theta}{r}\frac{\partial \rho}{\partial \theta} = 0. \tag{2.10}$$

The four components of the linearised Ohm's law are given by

$$\tilde{J}_r = -\frac{\sigma}{c}[c\tilde{E}_r + B_\phi \tilde{V}_\theta + \tilde{B}_\phi V_\theta - \tilde{B}_\theta V_\phi - B_\theta \tilde{V}_\phi] \tag{2.11}$$

$$\tilde{J}_\theta = -\frac{\sigma}{c}[c\tilde{E}_\theta + B_r \tilde{V}_\phi + \tilde{B}_r V_\phi - \tilde{B}_\phi V_r - B_\phi \tilde{V}_r] \tag{2.12}$$

$$\tilde{J}_\phi = -\frac{\sigma}{c}[c\tilde{E}_\phi + B_\theta \tilde{V}_r + \tilde{B}_\theta V_r - \tilde{B}_r V_\theta - B_r \tilde{V}_\theta] \tag{2.13}$$

$$\tilde{J}_t = -\frac{\sigma}{c}[E_r \tilde{V}_r + \tilde{E}_r V_r + E_\theta \tilde{V}_\theta + \tilde{E}_\theta V_\theta + \tilde{E}_\phi V_\phi] \tag{2.14}$$

Physical quantities with tilde over them denote perturbed variables. As for the energy equation, we use the adiabatic law

$$\frac{\mathrm{d}}{\mathrm{d}t}[P\rho^{-\gamma}] = 0, \tag{2.15}$$

i.e we consider the plasma to be an ideal fluid with no heat exchange with its surroundings. It is also to be noted that the equilibrium solutions were derived for an incompressible plasma and this equation (2.15) is necessary only to perform the stability analysis (see Corbelli & Ciamponi 1990).

## 2.1 *Local Analysis*

The stability analysis is confined to the disk's inner region where instabilities are expected to arise (paper I). The presence of the instability is based on the turning behaviour of pressure profile at $R$ = 18 m (m = GM/$c^2$) where maximum free source of energy is available to derive the instability. In this paper, we perform a local analysis which implies that $\mathrm{k}L_P \gg 1$, where $L_p$ is the pressure scale length ($L_p^{-1} = 1/P(\mathrm{d}P/\mathrm{d}r)$) and $\kappa$ is the wave number (for our equilibrium model $\hat{L}_p = L_p/R = 4$). Following the Standard normal mode analysis, the general time dependent perturbations are written in the following form

$$\tilde{\psi}(r, \theta, \phi, t) = C \exp[i(\nu t + \kappa r + n\theta + m\phi)] \tag{2.16}$$

where $\kappa$, $n$ and $m$ are real numbers and $\nu$ is, in general, a complex number. As the perturbation in-the $\theta$ direction represents the structure of the modes in that direction and does not change the nature of the instability, the stability analysis is performed at the $\theta = \pi/2$ plane (equatorial plane) as a first step towards a more general analysis. For the sake of simplicity and to understand the nature of the instability, we consider the perturbation to be a radial one and leave the solution of the full set of equations to a future study. We further assume that the plasma moves only along the azimuthal direction ($V_\phi \neq 0$; $V_r$ , $V_\theta = 0$). This may be justified because the plasma motion at the inner boundary is primarily along the azimuthal direction.

Upon substituting the radial perturbations into the disk equations (2.1–2.10 and 2.15), the linearised perturbation equations in dimensionless form are written as

$$(i\omega + \hat{\sigma})\tilde{\hat{E}}_r - \hat{\sigma}\tilde{\hat{V}}_\phi - \hat{\sigma}\hat{V}_\phi \tilde{\hat{B}}_\theta = 0, \tag{2.17}$$

$$(i\omega + \hat{\sigma})\tilde{\hat{E}}_\theta + \frac{\mathrm{d}\tilde{\hat{B}}_\phi}{\mathrm{d}\alpha} + \frac{\tilde{\hat{B}}_\phi}{\alpha} + (\hat{\sigma}\hat{V}_\phi)\tilde{\hat{B}}_r = 0, \tag{2.18}$$

$$(i\omega + \hat{\sigma})\tilde{\hat{E}}_\phi - \frac{\mathrm{d}\tilde{\hat{B}}_\theta}{\mathrm{d}\alpha} - \frac{\tilde{\hat{B}}_\theta}{\alpha} + \hat{\sigma}\tilde{\hat{V}}_r = 0, \tag{2.19}$$

$$i\omega\tilde{\hat{B}}_r = 0, \tag{2.20}$$

$$i\omega\tilde{\hat{B}}_\theta - \frac{\tilde{\hat{E}}_\phi}{\alpha} - \frac{\mathrm{d}\tilde{\hat{E}}_\phi}{\mathrm{d}\alpha} = 0, \tag{2.21}$$

$$i\omega\tilde{\hat{B}}_\phi + \frac{\tilde{\hat{E}}_\theta}{\alpha} + \frac{\mathrm{d}\tilde{\hat{E}}_\theta}{\mathrm{d}\alpha} = 0, \tag{2.22}$$

$$i\omega\tilde{\hat{V}}_r + \hat{\sigma}\hat{V}_A^2\tilde{\hat{V}}_r - \frac{2\hat{V}_\phi}{\alpha}\tilde{\hat{V}}_\phi + \hat{\sigma}V_A^2\tilde{\hat{E}}_\phi + \left(\frac{(\gamma-1)\mathrm{d}P}{\rho c^2\,\mathrm{d}\alpha}\right)\tilde{\hat{\rho}} + C_s^2\frac{\mathrm{d}\tilde{\hat{\rho}}}{\mathrm{d}\alpha} = 0, \tag{2.23}$$

$$i\omega\tilde{\hat{V}}_\theta = 0, \tag{2.24}$$

$$i\omega\tilde{\hat{V}}_\phi + (\hat{\sigma}V_A^2)\tilde{\hat{V}}_\phi - \hat{\sigma}V_A^2(\tilde{\hat{E}}_r - \hat{B}_\theta\tilde{\hat{V}}_\phi) = 0, \tag{2.25}$$

$$i\omega\tilde{\hat{\rho}} + \left(\frac{2}{\alpha} + \frac{\mathrm{d}}{\mathrm{d}\alpha}\right)\tilde{\hat{V}}_r = 0. \tag{2.26}$$

Here the hat over the quantities represents the dimensionless variables ($\hat{E}_i = E_i/B_\theta$, $B_i = B_i/B_\theta$, $\tilde{\rho} = \tilde{\rho}/\rho$ and $\hat{V}_i = V_i/c$). In addition we have defined the other normalised quantities as shown below:

$$\begin{aligned} k &= \kappa R, \quad \alpha = r/R \\ \hat{\sigma} &= 4\pi\sigma R/c, \quad \omega = \nu R/c \\ V_a^2 &= \frac{B_\theta^2}{4\pi\rho c^2}, \quad C_s^2 = \frac{\gamma P}{\rho c^2}. \end{aligned} \tag{2.27}$$

where $V_A$ and $C_s$ represent the normalised Alfven and sound speeds respectively. It is clear from the above equations (2.20 and 2.24) that the perturbations along $B_r$ and $V_\theta$ are zero. The remaining equations which are eliminated in terms of the electric fields are given below.

$$\begin{aligned} Q_1\tilde{\hat{E}}_\theta &= 0, \\ Q_2\tilde{\hat{E}}_r - Q_3\tilde{\hat{E}}_\phi &= 0, \\ Q_5\tilde{\hat{E}}_\phi - Q_4\tilde{\hat{E}}_r &= 0, \end{aligned} \tag{2.28}$$

where the coefficients $Q_1$ to $Q_5$ are defined in Appendix B. It is also to be noted that the validity of the local approximation ($k\hat{L}_p \gg 1$) demands $k$ to be $\gg 1/4$.

Setting the determinant of the system of equations (2.28) to zero, we obtain a dispersion relation in the form given by

$$Q_1(Q_2Q_5 - Q_3Q_4) = 0. \tag{2.29}$$

It is apparent that there exists two distinct dispersion relations corresponding to $Q_1 = 0$ and $(Q_2Q_5 - Q_3Q_4)=0$ and both are algebraic relations. The roots to the above dispersion relations are in general complex. The real component of $\omega$ gives an oscillatory nature to the wave while the negative imaginary component characterizes the instability and determines the growth rate of the unstable modes.

## 3. Results and discussions

The dispersion relation corresponding to $Q_1 = 0$ can be written as

$$\omega^2 - i\omega\hat{\sigma} - (k^2 - \alpha^{-2} - 2ik\alpha^{-1}) = 0 \tag{3.1}$$

Separating $\omega$ into real and imaginary components, the solution is found to be,

$$\omega_r = \frac{2k}{\alpha\hat{\sigma}}, \tag{3.2}$$

$$\omega_i = 0.5\hat{\sigma}\left[1 \pm \left\{1 + \frac{4}{\hat{\sigma}^2}\left(k^2 + \frac{4k^2}{\alpha^2\hat{\sigma}^2} - \frac{1}{\alpha^2}\right)\right\}^{1/2}\right]. \tag{3.3}$$

This expression corresponds to the resistive electromagnetic mode which can arise due to finite conductivity. However within the domain of local approximation this mode is found to be stable.

The dispersion relation corresponding to $(Q_2Q_5 - Q_3 Q_4) = 0$ in a compact form can be written as,

$$A_1\omega^5 + iA_2\omega^4 + (A_3 + iA_4)\omega^3 + (A_5 + iA_6)\omega^2 + (A_7 + iA_8)\omega + (A_9 + iA_{10}) = 0, \tag{3.4}$$

where the coefficients $A_1$, $A_2$ , . . .etc are defined in Appendix C. This equation has five different roots. However, only two roots being complex are interesting to analyse and is solved analytically for two different approximations. Subsequently, the full dispersion relation is solved numerically.

Under the approximation, $\omega \ll 1$ and $\omega\hat{\sigma} \ll 1$, the higher powers of $\omega$ may be neglected and the dispersion relation (3.4) reduces to,

$$(A_7 + iA_8)\omega + (A_9 + iA_{10}) = 0. \tag{3.5}$$

Writing $\omega = \omega_r + i\omega_i$, the solution of (3.5) in compact notation is written as

$$\omega_r = -\frac{A_7A_9 + A_8A_{10}}{A_7^2 + A_8^2}, \tag{3.6}$$

$$\omega_i = -\frac{A_7A_{10} - A_8A_9}{A_7^2 + A_8^2}, \tag{3.7}$$

or explicitly

$$\omega_i = -\frac{2}{\alpha\hat{\sigma}V_a^2(1 + 4k^2\alpha^2)}\left[DP\left\{1 + 3k^2\alpha^2 + k^4\alpha^4 + \frac{\hat{V}_\phi^2}{(1 + V_a^2)}(2 + k^2\alpha^2 + k^4\alpha^4)\right\} - \frac{\alpha k^2 C_s^2}{2M^2}\Phi\right], \tag{3.8}$$

where

$$M = \frac{V_a}{C_s}$$

$$DP = \frac{(\gamma - 1)}{\rho c^2} \frac{\mathrm{d}P}{\mathrm{d}\alpha}$$

$$P = \rho\left(P_0 + \frac{MG}{r} - \frac{V^2}{2}\right) - \frac{B^2}{8\pi} = 0$$

$$\Phi = \frac{6(1 + k^2\alpha^2)}{1 + V_a^2}\hat{V}_\phi^2 M^2 + k^4\alpha^4(M^2 + 1) + 2k^2\alpha^2(M^2 + 1.5) + M^2 - 4, \tag{3.9}$$

where $M$ signifies the magnetic Mach number (see paper I for the meaning of other notations).

It is worthwhile to note that this root corresponds to Kelvin-Helmholtz (K-H) mode as it arises due to finite velocity gradient. It can be further seen that there exists a threshold value of $\mathrm{d}V_\phi/\mathrm{d}r$ for the mode to become unstable. However in this particular analysis this mode is found to be stable. Nevertheless, it would be appropriate to point out that the flow velocity of the fluid appears through the equilibrium pressure term in the radial motion of the fluid and the velocity shear implicitly present in this term could probably drive the instability in a non-local analysis.

### 3.1 *Magnetosonic Mode*

Under the approximation, $1 \leqslant \omega \leqslant \hat{\sigma}$ and $\omega\hat{\sigma} \geqslant 1$, the relation (3.4) simplifies to,

$$\omega^2 = -\frac{(A_7 + iA_8)}{A_3 + iA_4}. \tag{3.10}$$

Separating ω into real and imaginary parts, we obtain

$$\omega_r = -\frac{c}{2a\omega_i}, \tag{3.11}$$

$$\omega_i = \pm\left[\frac{b}{2a}\left\{1 \pm \left(1 + \frac{c^2}{b^2}\right)\right\}^{1/2}\right]^{1/2}, \tag{3.12}$$

where

$$a = A_3^2 + A_4^2,$$
$$b = A_3A_7 + A_4A_8,$$
$$c = A_4A_7 - A_8A_3. \tag{3.13}$$

Out of four roots for $\omega_i$ only two roots lead to instability and these are given by

$$\omega_i = -\left[\frac{b}{2a}\left\{1 \pm \left(1 + \frac{c^2}{b^2}\right)\right\}^{1/2}\right]^{1/2}. \tag{3.14}$$

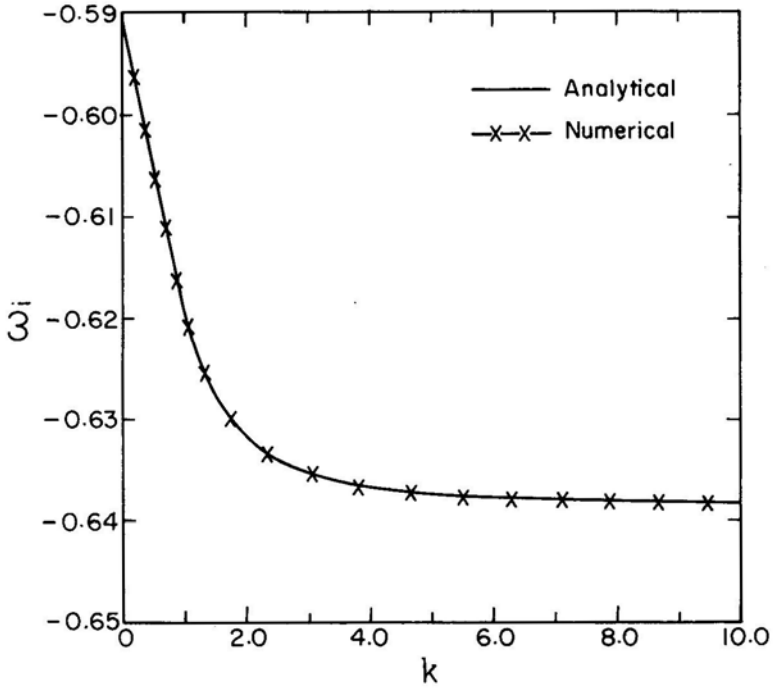


**Figure 2 (a).** Normalised growth rate.

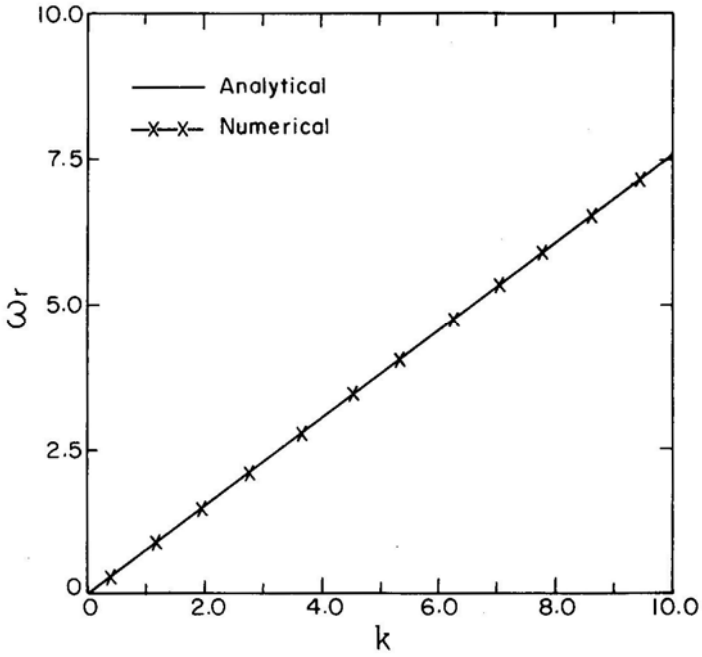


**Figure 2(b**). Normalised dispersion curve for magnetosonic instability. In figures 2(a) and 2(b), the solid line represents the results obtained analytically under the approximation $1 \leqslant \omega \leqslant \hat{\sigma}$ and $\omega\hat{\sigma} \geqslant 1$ whereas the -x-x-x line represents the numerical solution of the complete dispersion relation (equation 3.4).

For the root with plus sign inside the square bracket, $b$ should be positive which is satisfied for smaller $k$ values ($k \leqslant 0.5$) The other root with minus sign inside the square bracket requires $b$ to be negative for the instability to exist and this is valid for higher $k$ values ($k > 0.5$) The form of $\omega_i$ reveals that the instability is magnetosonic in nature and is propagating in the radially inward direction. We also find that this instability is independent of conductivity. The growth rate versus $k$ and the dispersion curve (Fig. 2) implies that the system is highly unstable against the magnetosonic instability for a wide range of $k$ spectrum. The growth rate of the mode decreases with $k$ and becomes constant for higher $k$ values. Thus, for our equilibrium structure, magnetosonic mode is the only candidate to destabilise the disk structure.

### 3.2 *Numerical Results*

The complete dispersion relation (3.4) is solved numerically using the complex routine ZROOTS from the Numerical Recipes (Press *et al* 1988). Out of the five possible roots only one gives rise to instability which is shown in Fig. 2 and corresponds to magnetosonic instability. It is also evident that the analytical and numerical results confirm very well with each other.

## 4. Conclusion

In most applications of plasma physics, plasma instabilities of various kinds play important roles. A plasma confined by a magnetic field is intrinsically unstable. Some examples from space plasmas include instabilities which produce nonthermal wave and particle accelerations in the magnetosphere. In the context of astrophysical plasmas, the instabilities lead to scattering and acceleration of fast particles leading to enhancement in radiation.

Our emphasis in astrophysical applications of MHD theory is the modeling of specific structure and analysis of their stability criterion. In the context of plasma accretion from a disk, an equilibrium configuration was worked out by Tripathy *et al.* (paper I) and in the present paper we discuss the stability of this equilibrium configuration. It is important to note that most of the instabilities occur near the magnetospheric boundary which is determined by the pressure balance condition which includes the magnetic pressure, inertial (ram) pressure and the gas pressure (see equation A5).

The present stability analysis considers radial perturbation of the resistive MHD equations ($\sigma \neq 0$). Implicitly we have also assumed that the thermal conductivity is zero (adiabatic equation of state) and that the viscosity is zero. The equilibrium pressure profile suggests the existence of K-H, resistive electromagnetic and magnetosonic modes. The K-H instability converts kinetic energy in mass flow into wave energy and the resistive MHD instability releases magnetic energy. The resistive effect is due to the finite electrical conductivity ($\sigma$). This allows the magnetic field lines to diffuse through the plasma. However, these two modes are found to be stable in this particular analysis whereas the magnetosonic instability can alter the disk structure significantly without disrupting the system. It becomes essential to study these instabilities in global approximation in which the existence of K-H and R-T mode instabilities is not ruled out.

## APPENDIX A

Here, we outline the boundary conditions that have been incorporated for the calculation of the magnetic field line configuration (Fig. 1).

In the presence of the magnetofluid with finite resistivity, magnetic lines of force can penetrate the accretion disk and hence the magnetic field lines should be continuous at the edge of the disk. Equating the disk field with the external dipolar field at the inner boundary, we obtain

$$B_1 = B_0\left(\frac{R}{r_{\text{in}}}\right)^{2+k}. \tag{A1}$$

The total magnetic field ($B_t$) is given by the some of the external and disk fields and the components are written in a non-dimensional form as

$$\frac{R^3 B_r}{\mu} = x^{-3}\cos\theta + x^{k-1}\sin^{k-1}\theta\cos\theta, \tag{A2}$$

$$\frac{R^3 B_\theta}{\mu} = 2x^{-3}\sin\theta + x^{k-1}\sin^{k}\theta, \tag{A3}$$

where $x = r/\text{m}$ and $x_{\text{in}} = r_{\text{in}}/\text{m}$.

This field line structure has been obtained by solving the equation

$$\frac{d\boldsymbol{X}}{ds} = \frac{\boldsymbol{B}}{|\boldsymbol{B}|}, \tag{A4}$$

and is plotted in Fig. 1 along with the condition that the total pressure at each point on both sides of the entire boundary be continuous. Mathematically, this condition can be expressed as,

$$\rho\left(P_0 + \frac{MG}{r} - \frac{V^2}{2}\right) - \frac{B_t^2}{8\pi} = 0. \tag{A5}$$

It is evident from Fig. 1 that inside the disk dipolar field lines are pushed in by the plasma accreted in the disk. Also, it is apparent that the field lines are connected with the distorted dipolar field lines at the surface of the disk and are continuous at the inner boundary.

## APPENDIX B

$$Q_1 = \omega^2 - i\omega\hat{\sigma} - (k^2 - \alpha^{-2} - 2ik\alpha^{-1}) \tag{B1}$$

$$Q_2 = \omega(1 + V_A^2 + i\omega\hat{\sigma}^{-1}) \tag{B2}$$

$$Q_3 = -\hat{V}_\phi(k - i\alpha^{-1}) \tag{B3}$$

$$Q_4 = -2\hat{V}_\phi\alpha^{-1}(1 + i\omega\hat{\sigma}^{-1}) \tag{B4}$$

$$Q_5 = \left[\frac{V_A^2}{\omega}(2k\alpha^{-1} + i(k^2 - \alpha^{-2}) - i\omega^2 - \hat{\sigma}\omega) + \frac{i}{\hat{\sigma}}\right] + \hat{\sigma}V_A^2 + \frac{2\hat{V}_\phi^2}{\alpha\omega}(k - i\alpha^{-1})$$
$$- \left[ikC_s^2 + \frac{(\gamma - 1)}{\rho c^2}\frac{dP}{d\alpha}\right]\frac{(k - 2i\alpha^{-1})}{\hat{\sigma}\omega^2}(2k\alpha^{-1} + i(k^2 - \alpha^{-2}) - i\omega^2 - \hat{\sigma}\omega). \tag{B5}$$

## APPENDIX C

$$A_1 = -\frac{1}{\hat{\sigma}^2} \tag{C1}$$

$$A_2 = \frac{2(1+V_A^2)}{\hat{\sigma}} \tag{C2}$$

$$A_3 = (1+V_A^2)^2 + \hat{\sigma}^{-2}[k^2(1+C_s^2) - 2\alpha^{-1}(DP) - \alpha^{-2}] \tag{C3}$$

$$A_4 = -k\hat{\sigma}^{-2}[2\alpha^{-1}(1+C_s^2) + DP] \tag{C4}$$

$$A_5 = -k\alpha^{-1}\hat{\sigma}^{-1}[2(1+2V_A^2) + (2+V_A^2)(2C_s^2 + \alpha DP)] \tag{C5}$$

$$A_6 = \hat{\sigma}^{-1}[(1+2V_A^2)(\alpha^{-2} - k^2) + (2+V_A^2)(2\alpha^{-1}DP - k^2C_s^2)] \tag{C6}$$

$$A_7 = (1+V_A^2)[2\alpha^{-1}DP + V_A^2\alpha^{-2} - k^2(V_A^2 + \hat{\sigma}^{-2}C_s^2)] + 2V_A^2\hat{V}_\phi^2\alpha^{-2} + C_s^2k^2(\alpha\hat{\sigma})^{-2}[5 - k^2\alpha^2] + 2k^2\alpha^{-1}\hat{\sigma}^{-2}DP[2 - k^{-2}\alpha^{-2}] \tag{C7}$$

$$A_8 = (1+V_A^2)\left[\frac{2k}{\alpha}(V_A^2 + C_s^2) + kDP\right] + \frac{2k}{\alpha}\left[2k^2C_s^2 + V_A^2\hat{V}_\phi^2\right] - \frac{k}{\alpha^3\hat{\sigma}^2}[2C_s^2 + \alpha DP(5 - k^2\alpha^3)] \tag{C8}$$

$$A_9 = (1+V_A^2)\frac{k}{\hat{\sigma}\alpha^2}\left[DP(k^2\alpha^2 - 5) - \frac{2C_s^2}{\alpha}(1 - 2k^2\alpha^2)\right] \tag{C9}$$

$$A_{10} = \frac{(1+V_A^2)}{\alpha^3\hat{\sigma}^{-1}}[2DP(1 - 2k^2\alpha^2) + \alpha k^2C_s^2(k^2\alpha^2 - 5)] \tag{C10}$$

## References


Anzer, U., Börner, G. 1980, *Astr. Astrophys*., **83**, 183.
Anzer, U., Börner, G. 1983, *Astr. Astrophys.*, **122**, 73.
Chandrasekhar, S. 1961, *Hydrodynamic and Hydromagnetic Stability,* (Oxford University Press, London).
Choudhury, S. R., Lovelace, R. V. E. 1986, *Astrophys. J*., **302**, 188.
Corbelli, E., Torricelli-Ciamponi, G. 1990, *Phys. Fluids*, *B*, **2**, 828.
Ghosh, P., Lamb, F. K. 1978, *Astrophys. J. Lett*, **223**, L83.
Press, W. H., Flannery, B. P., Teukolsky, S. A., Vetterling, W. T. 1988, *Numerical Recipes: The art of scientific computing,* (Cambridge University Press, New York).
Pietrini, P., Torricelli-Ciamponi, G. 1989, *Phys. Fluids B*, **1**, 923.
Prasanna, A. R. 1991, *Pramana–J. Phys*., **36**, 445.
Scharlemann, E. T. 1978, *Astrophys. J*., **219**, 617.
Shields, G. A., Wheeler, J. C. 1976, *Astrophys. J*., **17**, 69.
Taam, R. E., van den Heuvel, E. P. J. 1986, *Astrophys. J*., **305**, 235.
Tripathy, S. C, Prasanna, A. R., Das A. C. 1990, *Mon. Not. R. astr. Soc*., **246**, 384, (paper I).
Wiita, P. J. 1985, *Phys. Reports*, **219**, 617.